Available online at www.sciencedirect.com
SCIENCE DIRECT®
Journal of Computational Physics 194 (2004) 773–794
JOURNAL OF COMPUTATIONAL PHYSICS
www.elsevier.com/locate/jcp

An efficient, high-order perturbation approach for flow in random porous media via Karhunen–Loève and polynomial expansions

Dongxiao Zhang *, Zhiming Lu

Hydrology, Geochemistry, and Geology Group, EES-6, MS T003, Los Alamos National Laboratory, P.O. Box 1663, Los Alamos, NM 87545, USA

Received 23 May 2003; received in revised form 25 August 2003; accepted 30 September 2003

Abstract

In this study, we attempt to obtain higher-order solutions of the means and (co)variances of hydraulic head for saturated flow in randomly heterogeneous porous media on the basis of the combination of Karhunen–Loève decomposition, polynomial expansion, and perturbation methods. We first decompose the log hydraulic conductivity $Y = \ln K_s$ as an infinite series on the basis of a set of orthogonal Gaussian standard random variables $\{\xi_i\}$. The coefficients of the series are related to eigenvalues and eigenfunctions of the covariance function of log hydraulic conductivity. We then write head as an infinite series whose terms $h^{(n)}$ represent head of nth order in terms of σ_Y, the standard deviation of Y, and derive a set of recursive equations for $h^{(n)}$. We then decompose $h^{(n)}$ with polynomial expansions in terms of the products of n Gaussian random variables. The coefficients in these series are determined by substituting decompositions of Y and $h^{(n)}$ into those recursive equations. We solve the mean head up to fourth-order in σ_Y and the head variances up to third-order in σ_Y^2. We conduct Monte Carlo (MC) simulation and compare MC results against approximations of different orders from the moment-equation approach based on Karhunen–Loève decomposition (KLME). We also explore the validity of the KLME approach for different degrees of medium variability and various correlation scales. It is evident that the KLME approach with higher-order corrections is superior to the conventional first-order approximations and is computationally more efficient than the Monte Carlo simulation.

Keywords: Monte Carlo simulations; Heterogeneity; Uncertainty; Higher-order approximation; Karhunen–Loève decomposition

1. Introduction

Owing to heterogeneity of geological formations and incomplete knowledge of medium properties, the medium properties may be treated as random space functions and the equations describing flow and

* Corresponding author. Tel.: +505-667-3541; fax: +505-665-8737.
E-mail address: donzhang@lanl.gov (D. Zhang).

0021-9991/$ - see front matter © 2003 Elsevier Inc. All rights reserved.
doi:10.1016/j.jcp.2003.09.015

transport in these formations become stochastic. Stochastic approaches to flow and transport in heterogeneous porous media have been extensively studied in the last two decades, and many stochastic models have been developed [3,5,6,30].

Monte Carlo (MC) simulation is a conceptually straightforward method for solving these stochastic partial differential equations. It entails generating a large number of equally likely random realizations of the parameter fields, solving deterministic flow and transport equations for each realization, and averaging the results over all realizations to obtain sample moments of the solution. This approach has the advantages of applying to a broad range of both linear and nonlinear flow and transport problems. But, it also has a number of potential drawbacks [15,26]. A major disadvantage of the Monte Carlo method, among others, is the requirement for large computational effort. To properly resolve high frequency space–time fluctuations in random parameters, it is necessary to employ fine numerical grids in space–time. Therefore, computational effort for each realization is usually large, especially if both physical and chemical heterogeneities, as well as uncertainties in initial and boundary conditions, are considered. To ensure the convergence of the sample output moments to their theoretical ensemble values, a large number of realizations are often required (typically a few thousand realizations, depending on the degree of medium heterogeneity), which poses a significant computational burden.

An alternative to Monte Carlo simulations is the approach based on moment equations, the essence of which is to derive a system of deterministic partial differential equations governing the statistical moments of the flow and transport quantities (usually the first two moments, mean and covariance), and then solve them analytically or numerically [1,4,5,7,14–17,21,22,24,27,29,30].

The moment equations are usually derived with the method of perturbation. In the perturbation-based approach, the medium properties, such as log hydraulic conductivity Y, can be written as $Y = \langle Y\rangle + Y'$, and similarly the dependent variables, such as hydraulic head h, can be decomposed as $h = \langle h\rangle + h'$. After substituting these decompositions into the original stochastic equations with some mathematical manipulation one obtains equations for mean head and head perturbation. The mean equation cannot be solved directly because it contains some cross-covariance functions between head and medium properties, such as $\langle Y'h'\rangle$. The equation for $\langle Y'h'\rangle$ in turn will involve some third-order terms. One can either write an implicit equation for the head perturbation or equivalently express it explicitly as integrals whose integrands contain Green's function and other higher-order cross-covariance terms. The head covariance equation is then formulated from the equation for head perturbation.

Similarly, one can expand hydraulic head as an infinite series in terms of the standard deviation of the medium property. More specifically, for saturated flow as considered in this study, head is expanded as an infinite series $h = \sum_{n=0}^{\infty} h^{(n)}$ in terms of σ_Y, the standard deviation of the log hydraulic conductivity. Substituting the decomposition into the original equations yields a series of recursive equations in which the equation for $h^{(n)}$ involves lower order terms $h^{(i)}$, $i = 1, 2, \ldots, n-1$. In most existing models, the mean head is approximated up to second-order in σ_Y, and the head (co)variance is approximated up to first-order in σ_Y^2, i.e., $C_h(\mathbf{x}, \mathbf{y}) = \langle h^{(1)}(\mathbf{x})h^{(1)}(\mathbf{y})\rangle$. In computing the head covariance up to first-order in σ_Y^2, one needs to solve deterministic equations that are similar to the original equation about $2N$ times (N being the number of grid nodes): N times for solving C_{Yh} and about N time for C_h. Including higher-order terms is possible, but it will increase the computational effort dramatically.

Though in many cases this approach works quite well for relatively large variations in the medium properties [18,20,26,32], this approach in general is restricted to small variabilities of medium properties.

In this study, we attempt to obtain higher-order terms of the mean and variance of head based on the combination of Karhunen–Loève decomposition and perturbation methods. The application of Karhunen–Loève decomposition to solving stochastic boundary value problems has been pioneered by Ghanem and his coauthors [8–13,25] and further developed by Xiu and Karniadakis [28]. The essence of their technique includes discretizing the independent random process (e.g., log hydraulic conductivity) using Karhunen–Loève expansion and representing the dependent stochastic process (hydraulic head or concentration) using

the polynomial chaos basis. The deterministic coefficients of the dependent process in the polynomial chaos expansion are governed by a set of coupled equations and calculated via a weighted residual procedure. Roy and Grilli [23] combined the Karhunen–Loève decomposition and the perturbation methods to solve the steady state flow equation and obtained the mean head to first-order in σ_Y and the head variance to first-order in σ_Y^2. In this study, we aim to derive and evaluate higher-order approximations for the mean and (co)variance of head. Specifically, with the combination of Karhunen–Loève decomposition and perturbation methods we evaluate the mean head up to fourth-order in σ_Y and the head variances up to third-order in σ_Y^2. We also explore the validity of this approach for different degrees of medium variability and various correlation scales through comparisons against Monte Carlo simulations.

2. Stochastic differential equations

We consider transient water flow in saturated media satisfying the following continuity equation and Darcy's law:

$$S_s \frac{\partial h(\mathbf{x},t)}{\partial t} + \nabla \cdot \mathbf{q}(\mathbf{x},t) = g(\mathbf{x},t), \tag{1}$$

$$\mathbf{q}(\mathbf{x},t) = -K_s(\mathbf{x})\nabla h(\mathbf{x},t), \tag{2}$$

subject to initial and boundary conditions

$$h(\mathbf{x},0) = H_0(\mathbf{x}), \quad \mathbf{x} \in D, \tag{3}$$

$$h(\mathbf{x},t) = H(\mathbf{x},t), \quad \mathbf{x} \in \Gamma_{\mathrm{D}}, \tag{4}$$

$$\mathbf{q}(\mathbf{x},t) \cdot \mathbf{n}(\mathbf{x}) = Q(\mathbf{x},t), \quad \mathbf{x} \in \Gamma_{\mathrm{N}}, \tag{5}$$

where $\mathbf{q}$ is the specific discharge (flux), $h(\mathbf{x},t)$ is hydraulic head, $H_0(\mathbf{x})$ is the initial head in the domain D, $H(\mathbf{x},t)$ is the prescribed head on Dirichlet boundary segments Γ_{D}, $Q(\mathbf{x},t)$ is the prescribed flux across Neumann boundary segments Γ_{N}, $\mathbf{n}(\mathbf{x}) = (n_1,\ldots,n_d)^{\mathrm{T}}$ is an outward unit vector normal to the boundary $\Gamma = \Gamma_{\mathrm{D}} \cup \Gamma_{\mathrm{N}}$, and S_s is the specific storage.

In this study, we treat $K_s(\mathbf{x})$ as a random function. Thus, Eqs. (1)–(5) become stochastic partial differential equations, whose solutions are no longer deterministic values but probability distributions or related statistical moments.

3. KL decomposition of log hydraulic conductivity

Let $Y(\mathbf{x},\omega) = \ln[K_s(\mathbf{x},\omega)]$ be a random process, where $\mathbf{x} \in D$ and $\omega \in \Omega$ (a probability space). Because the covariance function $C_Y(\mathbf{x},\mathbf{y}) = \langle Y'(\mathbf{x},\omega)Y'(\mathbf{y},\omega)\rangle$ is bounded, symmetric, and positive definite, it can be decomposed into [2]

$$C_Y(\mathbf{x},\mathbf{y}) = \sum_{n=1}^{\infty} \lambda_n f_n(\mathbf{x}) f_n(\mathbf{y}), \tag{6}$$

where λ_n and $f_n(\mathbf{x})$ are called eigenvalues and eigenfunctions, respectively, and $f_n(\mathbf{x})$ are orthogonal and deterministic functions that form a complete set [19]

$$\int_D f_n(\mathbf{x}) f_m(\mathbf{x}) \mathrm{d}\mathbf{x} = \delta_{nm}, \quad n, m \geqslant 1. \tag{7}$$

The mean-removed stochastic process $Y'(\mathbf{x}, \omega)$ can be expanded in terms of $f_n(\mathbf{x})$ as

$$Y'(\mathbf{x}, \omega) = \sum_{n=1}^{\infty} \xi_n(\omega) \sqrt{\lambda_n} f_n(\mathbf{x}), \tag{8}$$

where $\xi_n(\omega)$ are orthogonal Gaussian random variables with zero mean, i.e., $\langle \xi_n(\omega) \rangle = 0$, and $\langle \xi_n(\omega) \xi_m(\omega) \rangle = \delta_{nm}$. The expansion in Eq. (8) is called the Karhunen–Loève expansion. It can be verified that the covariance of $Y'(\mathbf{x}, \omega)$ defined in (8) is indeed C_Y. For convenience, thereafter, we suppress symbol ω in $Y'(\mathbf{x}, \omega)$ and in other dependent functions.

Eigenvalues and eigenfunctions of a covariance function $C_Y(\mathbf{x}, \mathbf{y})$ can be solved from the following Fredholm equation:

$$\int_D C_Y(\mathbf{x}, \mathbf{y}) f(\mathbf{x}) \mathrm{d}\mathbf{x} = \lambda f(\mathbf{y}). \tag{9}$$

For some special types of covariance functions, λ_n and $f_n(\mathbf{x})$ can be found analytically, as shown in Appendix A for a one-dimensional stochastic process with a covariance function $C_Y(x_1, y_1) = \sigma_Y^2 \exp(-|x_1 - y_1|/\eta)$, where σ_Y^2 and η are the variance and the correlation length of the process, respectively. For this case, the eigenvalues and their corresponding eigenfunctions can be expressed as

$$\lambda_n = \frac{2\eta\sigma_Y^2}{\eta^2 w_n^2 + 1} \tag{10}$$

and

$$f_n(x) = \frac{1}{\sqrt{(\eta^2 w_n^2 + 1)L/2 + \eta}} [\eta w_n \cos(w_n x) + \sin(w_n x)], \tag{11}$$

where w_n are positive roots of the characteristic equation

$$(\eta^2 w^2 - 1) \sin(wL) = 2\eta w \cos(wL). \tag{12}$$

Eq. (12) has infinite number of positive roots. Sorting these roots w_n in an increasing order, which yields a monotonically decreasing series of λ_n. From Eq. (6) or (8) we have $\sigma_Y^2 = \sum_{n=1}^{\infty} \lambda_n f_n^2(\mathbf{x})$. Integrating this equation yields $D\sigma_Y^2 = \sum_{n=1}^{\infty} \lambda_n$, where D is a measure of the domain size (length, area, or volume for 1D, 2D, or 3D domain, respectively), which means that the total variance σ_Y^2 is decomposed into an infinite summation of eigenvalues λ_n.

For problems in multidimension, if we assume that the covariance function $C_Y(\mathbf{x}, \mathbf{y})$ is separable, for example, $C_Y(\mathbf{x}, \mathbf{y}) = \sigma_Y^2 \exp(-|x_1 - y_1|/\eta_1 - |x_2 - y_2|/\eta_2)$ for a rectangular domain $D = \{(x_1, x_2) : 0 \leqslant x_1 \leqslant L_1, 0 \leqslant x_2 \leqslant L_2\}$, Eq. (9) can be solved independently for x_1 and x_2 directions to obtain eigenvalues $\lambda_n^{(1)}$ and $\lambda_n^{(2)}$, and eigenfunctions $f_n^{(1)}(x_1)$ and $f_n^{(2)}(x_2)$. These eigenvalues and eigenfunctions are then combined to form eigenvalues and eigenfunctions of C_Y:

$$\lambda_n = \frac{4\eta_1\eta_2\sigma_Y^2}{[\eta_1^2 (w_i^{(1)})^2 + 1][\eta_2^2 (w_j^{(2)})^2 + 1]}, \tag{13}$$

$$f_n(\mathbf{x}) = f_n(x_1, x_2) = f_i^{(1)}(x_1) f_j^{(2)}(x_2), \tag{14}$$

where $w_i^{(1)}$ and $w_j^{(2)}$ are two series of positive roots of (12) using parameters (L_1, η_1) and (L_2, η_2), respectively. Here we assume that indices i and j are mapping to index n in such a way that λ_n form a series whose terms are nonincreasing. From Eq. (12) it is noted that its solutions $w_n \sim n\pi/L$ for large n, which means that λ_n defined in (10) decreases at a rate of $1/n^2$ and thus λ_n defined in (13) for two-dimensional problems decrease at a rate of $1/(i^2 j^2)$. The convergence of series $\sum_{n=1}^{\infty} 1/n^2$ ensures the convergence of infinity series in Eq. (6). Thus Y' can be approximated by a finite number of terms in Eq. (8).

Eq. (8) provides an alternative way for random field generation. Once eigenvalues λ_n and their corresponding eigenfunctions f_n are found, a realization can be computed simply by independently sampling a certain number of values z_n from the standard Gaussian distribution $N(0,1)$ and then computing $\sum_{n=1}^{N} z_n \sqrt{\lambda_n} f_n(\mathbf{x})$, where N is the number of terms needed to generate realizations with a given accuracy. The number N depends on the ratio of correlation length to the domain size. This will be discussed further in Section 6.

Since eigenvalues $\sqrt{\lambda_n}$ and their eigenfunctions $f_n(\mathbf{x})$ always come together, in the following derivation, we define new functions $\tilde{f}_n(\mathbf{x}) = \sqrt{\lambda_n} f_n(\mathbf{x})$ and the tilde over f_n is dropped for simplicity.

4. KL-based moment equations

For simplicity, in this study we assume that all initial and boundary conditions are deterministic. We assume that the hydraulic conductivity $K(\mathbf{x})$ follows a log normal distribution, and work with the log-transformed variable $Y(\mathbf{x}) = \ln(K(\mathbf{x})) = \langle Y(\mathbf{x})\rangle + Y'(\mathbf{x})$. The mean log saturated hydraulic conductivity $\langle Y(\mathbf{x})\rangle$ represents a relatively smooth unbiased estimate of the unknown random function $Y(\mathbf{x})$. It may be estimated using standard geostatistical methods, such as kriging, which produce unbiased estimates that honor measurements and provide uncertainty measures for these estimates. Here we assume that the log saturated hydraulic conductivity field may be conditioned on some measurement points, which means that the field may be statistically inhomogeneous. In this case, the two-point covariance function $C_Y(\mathbf{x}, \mathbf{y})$ depends on the actual locations of two points $\mathbf{x}$ and $\mathbf{y}$ rather than their separation distance, and therefore, the eigenvalues and eigenfunctions of $C_Y(\mathbf{x}, \mathbf{y})$, in general, have to be solved numerically.

Because the variability of $h(\mathbf{x}, t)$ depends on the input variabilities, i.e., variability of $Y(\mathbf{x})$, one may express $h(\mathbf{x}, t)$ as an infinite series as $h(\mathbf{x}, t) = h^{(0)} + h^{(1)} + h^{(2)} + \cdots$ In this series, the order of each term is with respect to σ_Y, the standard deviation of $Y(\mathbf{x})$. After combining (1) and (2), substituting expansions of $h(\mathbf{x}, t)$ and $Y(\mathbf{x})$, and collecting terms at separate order, one can obtain the following equations with initial and boundary conditions that govern the hydraulic head at different order in σ_Y:

$$\nabla^2 h^{(0)}(\mathbf{x}, t) + \nabla\langle Y(\mathbf{x})\rangle \cdot \nabla h^{(0)}(\mathbf{x}, t) = -\frac{g(\mathbf{x}, t)}{K_G(\mathbf{x})} + \frac{S_s}{K_G(\mathbf{x})} \frac{\partial h^{(0)}(\mathbf{x}, t)}{\partial t}, \tag{15}$$

$$h^{(0)}(\mathbf{x}, 0) = H_0(\mathbf{x}), \quad \mathbf{x} \in D, \tag{16}$$

$$h^{(0)}(\mathbf{x}, t) = H(\mathbf{x}, t), \quad \mathbf{x} \in \Gamma_D, \tag{17}$$

$$\nabla h^{(0)}(\mathbf{x}, t) \cdot \mathbf{n}(\mathbf{x}) = -Q(\mathbf{x}, t)/K_G(\mathbf{x}), \quad \mathbf{x} \in \Gamma_N, \tag{18}$$

and for $m \geqslant 1$,

$$\nabla^2 h^{(m)}(\mathbf{x}, t) + \nabla\langle Y(\mathbf{x})\rangle \cdot \nabla h^{(m)}(\mathbf{x}, t) = \frac{S_s}{K_G(\mathbf{x})} \sum_{k=0}^{m} \frac{(-1)^k}{k!} [Y'(\mathbf{x})]^k \frac{\partial h^{(m-k)}(\mathbf{x}, t)}{\partial t} - \nabla Y'(\mathbf{x}) \cdot \nabla h^{(m-1)}(\mathbf{x}, t) - \frac{g(\mathbf{x}, t)}{m! K_G(\mathbf{x})} [-Y'(\mathbf{x})]^m, \tag{19}$$

$$h^{(m)}(\mathbf{x},0)=0,\quad \mathbf{x}\in D, \tag{20}$$

$$h^{(m)}(\mathbf{x},t)=0,\quad \mathbf{x}\in \Gamma_{\mathrm{D}}, \tag{21}$$

$$\nabla h^{(m)}(\mathbf{x},t)\cdot\mathbf{n}(\mathbf{x})=-\frac{Q(\mathbf{x},t)}{m!K_{\mathrm{G}}(\mathbf{x})}[-Y'(\mathbf{x})]^m,\quad \mathbf{x}\in \Gamma_{\mathrm{N}}. \tag{22}$$

We assume that $h^{(1)}(\mathbf{x},t)$ can be expanded with the following polynomial expansion in terms of the orthogonal Gaussian random variables ξ_n, $n=1,2,\ldots,$

$$h^{(1)}(\mathbf{x},t)=\sum_{n=1}^{\infty}\xi_n h_n^{(1)}(\mathbf{x},t), \tag{23}$$

where $h_n^{(1)}(\mathbf{x},t)$, $n=1,2,\ldots,$ are deterministic functions to be determined. There are two ways to determine $h_n^{(1)}(\mathbf{x},t)$. Multiplying ξ_n to Eq. (23) and taking expectation yields $h_n^{(1)}(\mathbf{x},t)=\langle\xi_n h^{(1)}(\mathbf{x},t)\rangle$, which means that $h_n^{(1)}(\mathbf{x},t)$ can be determined simply by multiplying ξ_n to Eqs. (19)–(22) with $m=1$, taking their expectation, and then solving for $\langle\xi_n h^{(1)}(\mathbf{x},t)\rangle$. Alternatively, substituting Eq. (23) and the expansion of $Y'(\mathbf{x})$ into Eqs. (19)–(22) with $m=1$ yields an infinite series in terms of ξ_n, whose summation equals to zero. For example, Eq. (19) becomes

$$\sum_{n=1}^{\infty}\xi_n\left[\nabla^2 h_n^{(1)}(\mathbf{x},t)+\nabla\langle Y(\mathbf{x})\rangle\cdot\nabla h_n^{(1)}(\mathbf{x},t)-\frac{S_s}{K_{\mathrm{G}}(\mathbf{x})}\left(\frac{\partial h_n^{(1)}(\mathbf{x},t)}{\partial t}-f_n(\mathbf{x})\frac{\partial h^{(0)}(\mathbf{x},t)}{\partial t}\right)\right.$$
$$\left.+\nabla f_n(\mathbf{x})\cdot\nabla h^{(0)}(\mathbf{x})-\frac{g(\mathbf{x},t)}{K_{\mathrm{G}}(\mathbf{x})}f_n(\mathbf{x})\right]=0. \tag{24}$$

Because of orthogonality of set ξ_n, $n=1,2,\ldots,$ all coefficients of this infinite series have to be zero, which leads to equations with initial and boundary conditions for $h_n^{(1)}(\mathbf{x},t)$:

$$\nabla^2 h_n^{(1)}(\mathbf{x},t)+\nabla\langle Y(\mathbf{x})\rangle\cdot\nabla h_n^{(1)}(\mathbf{x},t)=\frac{S_s}{K_{\mathrm{G}}(\mathbf{x})}\left[\frac{\partial h_n^{(1)}(\mathbf{x},t)}{\partial t}-f_n(\mathbf{x})\frac{\partial h^{(0)}(\mathbf{x},t)}{\partial t}\right]$$
$$-\nabla f_n(\mathbf{x})\cdot\nabla h^{(0)}(\mathbf{x})+\frac{g(\mathbf{x},t)}{K_{\mathrm{G}}(\mathbf{x})}f_n(\mathbf{x}), \tag{25}$$

$$h_n^{(1)}(\mathbf{x},0)=0,\quad \mathbf{x}\in D, \tag{26}$$

$$h_n^{(1)}(\mathbf{x},t)=0,\quad \mathbf{x}\in \Gamma_{\mathrm{D}}, \tag{27}$$

$$\nabla h_n^{(1)}(\mathbf{x},t)\cdot\mathbf{n}(\mathbf{x})=\frac{Q(\mathbf{x},t)}{K_{\mathrm{G}}(\mathbf{x})}f_n(\mathbf{x}),\quad \mathbf{x}\in \Gamma_{\mathrm{N}}. \tag{28}$$

Recalling the definition of $f_n(\mathbf{x})$, it is seen that all driving terms in Eqs. (25)–(28) are proportional to $\sqrt{\lambda_n}$, which decreases monotonically as n increases. This ensures that the magnitude of contribution of $h_n^{(1)}(\mathbf{x},t)$ to $h^{(1)}(\mathbf{x},t)$ decreases with n in general. This also clearly indicates that $h_n^{(1)}(\mathbf{x},t)$ are proportional to σ_Y, the standard deviation of log hydraulic conductivity.

To expand $h^{(2)}(\mathbf{x},t)$, we notice that by multiplying ξ_n to Eqs. (19)–(22) of $m=2$ and taking ensemble mean yields an equation with initial and boundary conditions for $\langle\xi_n h^{(2)}(\mathbf{x},t)\rangle$ that leads to the solution $\langle h^{(2)}(\mathbf{x},t)\xi_n\rangle\equiv 0$ for all $n\geqslant 1$, which means that $h^{(2)}(\mathbf{x},t)$ cannot be expanded in terms of ξ_n.

Note that the set $\{\xi_i\xi_j,\ i \geqslant j \geqslant 1\}$, are not orthogonal. For example, for any two elements of this set, $\xi_i\xi_i$ and $\xi_j\xi_j$, we have $\langle \xi_i\xi_i\xi_j\xi_j\rangle = 1 \neq 0$ for $i \neq j$. However, the set is linearly independent. In fact, $\mathrm{cov}(\xi_i\xi_j, \xi_m\xi_n) = \langle \xi_i\xi_j\xi_m\xi_n\rangle - \langle \xi_i\xi_j\rangle\langle \xi_m\xi_n\rangle = \delta_{im}\delta_{jn} + \delta_{in}\delta_{jm} \neq 0$ only if the set of subscripts $\{i,j\}$ is identical to the set $\{m,n\}$. Therefore, we can expand $h^{(2)}(\mathbf{x},t)$ as an infinite series in terms of $\xi_i\xi_j$, $i \geqslant j \geqslant 1$, i.e., $h^{(2)}(\mathbf{x},t) = \sum_{i\geqslant j\geqslant 1}^{\infty} \xi_i\xi_j\tilde{h}_{ij}^{(2)}(\mathbf{x},t)$, where $\tilde{h}_{ij}^{(2)}(\mathbf{x},t)$ are deterministic functions. Though $\xi_i\xi_j$ and $\xi_j\xi_i$ in the expansion are the same term, for convenience in our presentation, we split this term into two terms with the same coefficients, i.e., $h_{ij}^{(2)} = h_{ji}^{(2)} = \tilde{h}_{ij}^{(2)}/2$ for $i \neq j$ and $h_{ii}^{(2)} = \tilde{h}_{ii}^{(2)}$, thus $h^{(2)}(\mathbf{x},t)$ is formally written as

$$h^{(2)}(\mathbf{x},t) = \sum_{i,j=1}^{\infty} \xi_i\xi_j h_{ij}^{(2)}(\mathbf{x},t). \tag{29}$$

It can be verified that $\langle h^{(2)}(\mathbf{x},t)\xi_n\rangle \equiv 0$ for all $n \geqslant 1$. It is important to mention here that the second-order polynomial chaos expansion of Ghanem and Spanos [8], $\{\xi_i\xi_j - \delta_{ij},\ i,j = 1,2,\ldots\}$, or the second-order generalized polynomial chaos expansion of Xiu and Karniadakis [28], are orthogonal and may be used as a basis to expand $h^{(2)}(\mathbf{x},t)$. However, because $\langle \xi_i\xi_j - \delta_{ij}\rangle \equiv 0$, the expansion $h^{(2)}(\mathbf{x},t) = \sum_{i,j=1}^{\infty}(\xi_i\xi_j - \delta_{ij})$ $h_{ij}^{(2)}(\mathbf{x},t)$ results in $\langle h^{(2)}(\mathbf{x},t)\rangle \equiv 0$. On the other hand, if we take ensemble mean of Eqs. (19)–(22) with $m = 2$, we have in general $\langle h^{(2)}(\mathbf{x},t)\rangle \neq 0$ unless the medium is homogeneous, which means that the latter expansion does not satisfy equations Eqs. (19)–(22) of $m = 2$ for flow in heterogeneous media.

Substituting (29) as well as expansions of $Y'(\mathbf{x})$ and $h^{(1)}(\mathbf{x},t)$ into equations Eqs. (19)–(22) of $m = 2$ yields an infinite series in terms of $\xi_i\xi_j$ whose summation equals to zero. Because elements in the set $\{\xi_i\xi_j,\ i,j = 1,2,\ldots\}$ are linearly independent, all coefficients of this infinite series have to be zero, which leads to equations for $h_{ij}^{(2)}(\mathbf{x},t)$:

$$\begin{aligned}\nabla^2 h_{ij}^{(2)}(\mathbf{x},t) + \nabla\langle Y(\mathbf{x})\rangle\cdot\nabla h_{ij}^{(2)}(\mathbf{x},t) = \frac{S_s}{K_{\mathrm{G}}(\mathbf{x})}\Bigg[&\frac{\partial h_{ij}^{(2)}(\mathbf{x},t)}{\partial t} - \frac{1}{2}f_i(\mathbf{x})\frac{\partial h_j^{(1)}(\mathbf{x},t)}{\partial t} - \frac{1}{2}f_j(\mathbf{x})\frac{\partial h_i^{(1)}(\mathbf{x},t)}{\partial t}\\ &+ \frac{1}{2}f_i(\mathbf{x})f_j(\mathbf{x})\frac{\partial h^{(0)}(\mathbf{x},t)}{\partial t}\Bigg] - \frac{g(\mathbf{x})}{2K_{\mathrm{G}}(\mathbf{x})}f_i(\mathbf{x})f_j(\mathbf{x})\\ &- \frac{1}{2}\nabla f_i(\mathbf{x})\cdot\nabla h_j^{(1)}(\mathbf{x},t) - \frac{1}{2}\nabla f_j(\mathbf{x})\cdot\nabla h_i^{(1)}(\mathbf{x},t),\end{aligned} \tag{30}$$

$$h_{ij}^{(2)}(\mathbf{x},0) = 0, \quad \mathbf{x}\in D, \tag{31}$$

$$h_{ij}^{(2)}(\mathbf{x},t) = 0, \quad \mathbf{x}\in \Gamma_{\mathrm{D}}, \tag{32}$$

$$\nabla h_{ij}^{(2)}(\mathbf{x},t)\cdot\mathbf{n}(\mathbf{x}) = -\frac{Q(\mathbf{x},t)}{2K_{\mathrm{G}}(\mathbf{x})}f_i(\mathbf{x})f_j(\mathbf{x}), \quad \mathbf{x}\in\Gamma_{\mathrm{N}}. \tag{33}$$

Note that the term $\nabla Y'\cdot\nabla h^{(1)}$ in the second-order equations of (19)–(22) with $m = 2$ can be written either as $\sum_{i,j=1}^{\infty}\nabla f_i(\mathbf{x})\cdot\nabla h_j^{(1)}$ or equivalently as $\sum_{i,j=1}^{\infty}\nabla f_j(\mathbf{x})\cdot\nabla h_i^{(1)}$. To make $h_{ij}^{(2)}$ symmetric, we have written the term that corresponds to $\nabla Y'\cdot\nabla h^{(1)}$ as a half of $\nabla f_i(\mathbf{x})\cdot\nabla h_j^{(1)} + \nabla f_j(\mathbf{x})\cdot\nabla h_i^{(1)}$ in Eq. (30). A similar treatment has been done for term $Y'\partial h^{(1)}/\partial t$. Because both f_i and $h_i^{(1)}$ are proportional to $\sqrt{\lambda_i}$, it is seen from Eqs. (30)–(33) that all driving terms are proportional to $\sqrt{\lambda_i\lambda_j}$, i.e., proportional to σ_Y^2. The decrease of $\sqrt{\lambda_i\lambda_j}$ as i and j increase ensures that Eqs. (30)–(33) need to be solved for only a small number of times. In addition, because of symmetry, we only need to solve $h_{ij}^{(2)}(\mathbf{x},t)$ for $i \geqslant j$.

By multiplying $\xi_i\xi_j$ to the third-order equations of (19)–(22) and taking expectation, one obtains equations for $\langle \xi_i\xi_j h^{(3)}(\mathbf{x},t)\rangle$, which lead to a trivial solution $\langle \xi_i\xi_j h^{(3)}(\mathbf{x},t)\rangle = 0$. This implies that $h^{(3)}(\mathbf{x},t)$

cannot be expanded in terms of $\xi_i\xi_j$. However, if we multiply ξ_n or $\xi_i\xi_j\xi_k$ to (19)–(22) of $m = 3$ and take their expectations, respectively, trivial solutions for $\langle \xi_n h^{(3)}(\mathbf{x},t)\rangle$ and $\langle \xi_i\xi_j\xi_k h^{(3)}(\mathbf{x},t)\rangle$ do not exist, which means that $h^{(3)}(\mathbf{x},t)$ may be expanded as

$$h^{(3)}(\mathbf{x},t) = \sum_{n=1}^{\infty} \xi_n h_n^{(3)}(\mathbf{x},t) + \sum_{i,j,k=1}^{\infty} \xi_i\xi_j\xi_k h_{ijk}^{(3)}(\mathbf{x},t). \tag{34}$$

Substituting Eq. (34) and decompositions of Y', $h^{(1)}$ and $h^{(2)}$ into Eqs. (19)–(22) of $m = 3$ yields an infinite series whose summation is zero. Because elements of the combined set of $\{\xi_n,\ n = 1,2,\ldots\}$ and $\{\xi_i\xi_j\xi_k,\ i,j,k = 1,2,\ldots\}$ are linearly independent, all coefficients of the infinite series must be zero, which immediately leads to homogeneous equations for $h_n^{(3)}(\mathbf{x},t)$ with zero driving forces that yield $h_n^{(3)}(\mathbf{x},t) \equiv 0$, for all n. $h_{ijk}^{(3)}(\mathbf{x},t)$ satisfy the following equation with initial and boundary conditions:

$$\begin{aligned}\nabla^2 h_{ijk}^{(3)}(\mathbf{x},t) + \nabla\langle Y(\mathbf{x})\rangle\cdot\nabla h_{ijk}^{(3)}(\mathbf{x},t) = \frac{S_s}{K_{\mathrm{G}}(\mathbf{x})}\Bigg[&\frac{\partial h_{ijk}^{(3)}(\mathbf{x},t)}{\partial t} - \frac{1}{3}\sum_{P_{ijk}} f_i(\mathbf{x})\frac{\partial h_{jk}^{(2)}(\mathbf{x},t)}{\partial t}\\ &+ \frac{1}{6}\sum_{P_{ijk}} f_i(\mathbf{x})f_j(\mathbf{x})\frac{\partial h_k^{(1)}}{\partial t} - \frac{1}{6}f_i(\mathbf{x})f_j(\mathbf{x})f_k(\mathbf{x})\frac{\partial h^{(0)}(\mathbf{x},t)}{\partial t}\Bigg]\\ &+ \frac{g(\mathbf{x})}{6K_{\mathrm{G}}(\mathbf{x})}f_i(\mathbf{x})f_j(\mathbf{x})f_k(\mathbf{x}) - \frac{1}{3}\sum_{P_{ijk}}\nabla f_i(\mathbf{x})\cdot\nabla h_{jk}^{(2)}(\mathbf{x},t),\end{aligned} \tag{35}$$

$$h_{ijk}^{(3)}(\mathbf{x},0) = 0, \quad \mathbf{x}\in D, \tag{36}$$

$$h_{ijk}^{(3)}(\mathbf{x},t) = 0, \quad \mathbf{x}\in \Gamma_{\mathrm{D}}, \tag{37}$$

$$\nabla h_{ijk}^{(3)}(\mathbf{x},t)\cdot\mathbf{n}(\mathbf{x}) = \frac{Q(\mathbf{x},t)}{6K_{\mathrm{G}}(\mathbf{x})}f_i(\mathbf{x})f_j(\mathbf{x})f_k(\mathbf{x}), \quad \mathbf{x}\in\Gamma_{\mathrm{N}}, \tag{38}$$

where summation $\sum$ is over a subset of the permutation of $\{i,j,k\}$, in which repeated terms are excluded. For example, $\sum_{P_{ijk}}\nabla f_i\cdot\nabla h_{jk}^{(2)} = \nabla f_i\cdot\nabla h_{jk}^{(2)} + \nabla f_j\cdot\nabla h_{ik}^{(2)} + \nabla f_k\cdot\nabla h_{ij}^{(2)}$. Here the rest of terms, such as $\nabla f_i\cdot\nabla h_{kj}^{(2)}$ which is the same as $\nabla f_i\cdot\nabla h_{jk}^{(2)}$, are not included.

It should be noted that coefficients $h_n^{(3)}$ in (34) are zero, simply because elements in set $\{\xi_n,\ n = 1,2,\ldots\}$ and those in set $\{\xi_i\xi_j\xi_k,\ i,j,k = 1,2,\ldots\}$ are linearly independent. It is easy to show that, in general, we can assume that $h^{(m)}(\mathbf{x},t)$ can be expanded as

$$h^{(m)}(\mathbf{x},t) = \sum_{i_1,i_2,\ldots,i_m=1}^{\infty}\left(\prod_{j=1}^{m}\xi_{i_j}\right)h_{i_1,i_2,\ldots,i_m}^{(m)}(\mathbf{x},t). \tag{39}$$

Substituting this expansion and decompositions of Y' and all lower order terms $h^{(i)}$, $i = 1,2,\ldots,m-1$, into (19)–(22), one has

$$\begin{aligned}\nabla^2 h_{i_1,i_2,\ldots,i_m}^{(m)}(\mathbf{x},t) + \nabla\langle Y(\mathbf{x})\rangle\cdot\nabla h_{i_1,i_2,\ldots,i_m}^{(m)}(\mathbf{x},t) = &\frac{S_s}{K_{\mathrm{G}}(\mathbf{x})}\sum_{k=0}^{m}(-1)^k\frac{(m-k)!}{m!}\\ &\times\sum_{P_{i_1,\ldots,i_m}}\left(\prod_{j=1}^{k}f_{i_j}\right)\frac{\partial h_{i_{k+1},\ldots,i_m}^{(m-k)}(\mathbf{x},t)}{\partial t} + \frac{(-1)^{m+1}g(\mathbf{x})}{m!K_{\mathrm{G}}(\mathbf{x})}\\ &\times\prod_{j=1}^{m}f_{i_j}(\mathbf{x}) - \frac{1}{m}\sum_{P_{i_1,\ldots,i_m}}\nabla f_{i_1}(\mathbf{x})\cdot\nabla h_{i_2,\ldots,i_m}^{(m-1)}(\mathbf{x},t),\end{aligned} \tag{40}$$

$$h^{(m)}_{i_1,i_2,\ldots,i_m}(\mathbf{x},0)=0,\quad \mathbf{x}\in D, \tag{41}$$

$$h^{(m)}_{i_1,i_2,\ldots,i_m}(\mathbf{x},t)=0,\quad \mathbf{x}\in \Gamma_{\mathrm{D}}, \tag{42}$$

$$\nabla h^{(m)}_{i_1,i_2,\ldots,i_m}(\mathbf{x},t)\cdot\mathbf{n}(\mathbf{x})=\frac{(-1)^{m+1}Q(\mathbf{x},t)}{m!K_{\mathrm{G}}(\mathbf{x})}\prod_{j=1}^{m}f_{i_j}(\mathbf{x}),\quad \mathbf{x}\in\Gamma_{\mathrm{N}}. \tag{43}$$

We solve equations (40)–(43) up to fifth-order, i.e., $m=5$. Once we solved $h^{(0)}(\mathbf{x},t)$, $h^{(1)}_n(\mathbf{x},t)$, $h^{(2)}_{ij}(\mathbf{x},t)$, $h^{(3)}_{ijk}(\mathbf{x},t)$, $h^{(4)}_{ijkl}(\mathbf{x},t)$, and $h^{(5)}_{ijklm}(\mathbf{x},t)$, we can directly compute mean head and head covariance without solving equations for head covariance and the cross-covariance between log hydraulic conductivity and head that are required in the traditional moment-equation-based approaches. Up to fifth-order in σ_Y, head is approximated by

$$h(\mathbf{x},t)\approx\sum_{i=0}^{5}h^{(i)}(\mathbf{x},t), \tag{44}$$

which leads to an expression for mean head

$$\langle h(\mathbf{x},t)\rangle\approx\sum_{i=0}^{5}\langle h^{(i)}(\mathbf{x},t)\rangle=h^{(0)}(\mathbf{x},t)+\sum_{i=1}^{\infty}h^{(2)}_{ii}(\mathbf{x},t)+3\sum_{i,j=1}^{\infty}h^{(4)}_{iijj}(\mathbf{x},t). \tag{45}$$

It is seen that $\langle h^{(0)}(\mathbf{x},t)\rangle\equiv h^{(0)}(\mathbf{x},t)$ is the mean head solution up to first-order in σ_Y, the second term on the right hand side of (45) represents the second-order (or third-order) correction to the first-order mean head, and the third term is the fourth-order (or fifth-order) correction.

From (44) and (45), one can write the perturbation term up to fifth-order

$$h'(\mathbf{x},t)=h(\mathbf{x},t)-\langle h(\mathbf{x},t)\rangle\approx\sum_{i=1}^{5}h^{(i)}(\mathbf{x},t)-\langle h^{(2)}(\mathbf{x},t)\rangle-\langle h^{(4)}(\mathbf{x},t)\rangle, \tag{46}$$

where $\langle h^{(2)}\rangle=\sum_{i=1}^{\infty}h^{(2)}_{ii}$ and $\langle h^{(4)}\rangle=3\sum_{i,j=1}^{\infty}h^{(4)}_{iijj}$. Eq. (46) leads to the cross-covariance between log hydraulic conductivity and head up to third-order in σ_Y^2 (or, sixth-order in σ_Y),

$$C_{Yh}(\mathbf{x};\mathbf{y},\tau)=\sum_{n=1}^{\infty}f_n(\mathbf{x})h^{(1)}_n(\mathbf{y},\tau)+3\sum_{i,j=1}^{\infty}f_i(\mathbf{x})h^{(3)}_{ijj}(\mathbf{y},\tau)+\sum_{i,j,k,l,m,n=1}^{\infty}\xi_{ijklmn}f_i(\mathbf{x})h^{(5)}_{jklmn}(\mathbf{y},\tau), \tag{47}$$

and the head covariance

$$\begin{aligned}C_h(\mathbf{x},t;\mathbf{y},\tau)=&\sum_{i=1}^{\infty}h^{(1)}_i(\mathbf{x},t)h^{(1)}_i(\mathbf{y},\tau)+2\sum_{i,j=1}^{\infty}h^{(2)}_{ij}(\mathbf{x},t)h^{(2)}_{ij}(\mathbf{y},\tau)+3\sum_{i,j=1}^{\infty}h^{(1)}_i(\mathbf{x},t)h^{(3)}_{ijj}(\mathbf{y},\tau)\\&+3\sum_{i,j=1}^{\infty}h^{(1)}_i(\mathbf{y},\tau)h^{(3)}_{ijj}(\mathbf{x},t)+\sum_{i,j,k,l,m,n=1}^{\infty}\xi_{ijklmn}\Big[h^{(1)}_i(\mathbf{x},t)h^{(5)}_{jklmn}(\mathbf{y},\tau)+h^{(2)}_{ij}(\mathbf{x},t)h^{(4)}_{klmn}(\mathbf{y},\tau)\\&+h^{(3)}_{ijk}(\mathbf{x},t)h^{(3)}_{lmn}(\mathbf{y},\tau)+h^{(4)}_{ijkl}(\mathbf{x},t)h^{(2)}_{mn}(\mathbf{y},\tau)+h^{(5)}_{ijklm}(\mathbf{x},t)h^{(1)}_n(\mathbf{y},\tau)\Big]\\&-\langle h^{(2)}(\mathbf{x},t)\rangle\langle h^{(4)}(\mathbf{y},\tau)\rangle-\langle h^{(4)}(\mathbf{x},t)\rangle\langle h^{(2)}(\mathbf{y},\tau)\rangle,\end{aligned} \tag{48}$$

where $\xi_{ijklmn}=\langle\xi_i\xi_j\xi_k\xi_l\xi_m\xi_n\rangle$ for brevity. Because $\{\xi_n,\ n=1,2,\ldots\}$ is a set of independent Gaussian random variables, the $\langle\xi_i\xi_j\xi_k\xi_l\xi_m\xi_n\rangle$ term can be easily evaluated by counting the occurrence of each ξ and

using relationships $\langle \xi_i^{2k+1} \rangle = 0$ and $\langle \xi_i^{2k} \rangle = (2k-1)!!$. For instance, $\langle \xi_1 \xi_2^2 \xi_3^3 \rangle = \langle \xi_1 \rangle \langle \xi_2^2 \rangle \langle \xi_3^3 \rangle = 0$ and $\langle \xi_1^2 \xi_2^4 \rangle = \langle \xi_1^2 \rangle \langle \xi_2^4 \rangle = 1!! \cdot 3!! = 3$. Eq. (48) leads to the head variance up to third-order in σ_Y^2 (or, sixth-order in σ_Y)

$$\begin{aligned}\sigma_h^2(\mathbf{x},t) = {} & \sum_{i=1}^{\infty} [h_i^{(1)}(\mathbf{x},t)]^2 + 2\sum_{i,j=1}^{\infty} [h_{ij}^{(2)}(\mathbf{x},t)]^2 + 6\sum_{i,j=1}^{\infty} h_i^{(1)}(\mathbf{x},t) h_{ijj}^{(3)}(\mathbf{x},t) \\ & + \sum_{i,j,k,l,m,n=1}^{\infty} \xi_{ijklmn} \left[2h_i^{(1)}(\mathbf{x},t) h_{jklmn}^{(5)}(\mathbf{x},t) + 2h_{ij}^{(2)}(\mathbf{x},t) h_{klmn}^{(4)}(\mathbf{x},t) + h_{ijk}^{(3)}(\mathbf{x},t) h_{lmn}^{(3)}(\mathbf{x},t) \right] \\ & - 2\langle h^{(2)}(\mathbf{x},t) \rangle \langle h^{(4)}(\mathbf{x},t) \rangle. \end{aligned} \tag{49}$$

Here the first term in the right-hand side of (49) represents the head variance up to first-order in σ_Y^2, the second and third terms are second-order (in σ_Y^2) corrections, and the rest terms are the third-order (in σ_Y^2) corrections. Once we solved for the head terms, the flux moments can be derived from (2).

5. Issues on numerical implementation

5.1. Numerical solution of Fredholm equations

In Section 3, we discussed the solution of the Fredholm equation, i.e., Eq. (9), in a special case of separable covariance functions of log hydraulic conductivity $Y(\mathbf{x})$ in a rectangular domain. In general, however, the simulated flow domain may be irregularly shaped and the covariance function may not be separable. In this case, the eigenvalues and their corresponding eigenfunctions have to be solved numerically. Examples of such numerical algorithms include iterative methods and a Galerkin-type method. The latter is described in [8]. The basic idea in this algorithm is to choose a complete set of functions $\{\phi_i(\mathbf{x}),\ i = 1, 2, \ldots\}$ in the Hilbert space, express the eigenfunctions f_n to be sought as truncated (finite) linear combinations $f_n = \sum_{i=1}^{N} a_{in}\phi_i(\mathbf{x})$, and to determine coefficients a_{in} by forcing truncating errors to be orthogonal to $\phi_i(\mathbf{x}),\ i = 1, 2, \ldots, N$. The readers are referred to [8] for details.

In the case that some measurements of $Y(\mathbf{x})$ are available, one may wish to condition the $Y(\mathbf{x})$ field on these measurements. This can be done, for example, by kriging. The covariance function of the conditional $Y(\mathbf{x})$ field between any two points in general depends on actual locations of these points rather than the separation distance between two points. Roy and Grilli [23] developed an algorithm for computing eigenfunctions of conditional covariance of log hydraulic conductivity in a rectangular domain by assuming that the unconditional covariance function is separable. Once the eigenvalues λ_n and eigenfunctions f_n of the unconditional $Y(\mathbf{x})$ are found (analytically), one can expands the eigenfunctions of the conditional $Y(\mathbf{x})$ using f_n (which form a complete orthogonal basis), and determine the coefficients of expansions by solving an algebraic eigenvalue problem.

5.2. Computational efficiency of the KL-based approach

As mentioned in the introduction, for the conventional moment-equation-based approaches, to obtain the head covariance up to first-order in σ_Y^2, one needs to solve both the cross-covariance $C_{Yh}(\mathbf{x};\mathbf{y},\tau)$ and head covariance $C_h(\mathbf{x},t;\mathbf{y},\tau)$. At each time, both require to solve for N times an algebraic equation of N unknows (N being the number of grid nodes). Therefore, one needs to solve the algebraic equation with N unknows for about $2N$ times. If we want to find higher-order corrections, the computational burden increases drastically. For instance, to obtain the head variance up to second-order in σ_Y^2, one may need to solve equations for terms such as $\langle Y'(\mathbf{x})Y'(\mathbf{y})h'(\mathbf{z},\theta) \rangle$ (where θ is time), which in general requires solving linear algebraic equations of N unknows N^2 time for each θ.

In the KL-based perturbation approach, instead of solving the covariance equations we solve for the head terms $h^{(m)}_{i_1,i_2,\ldots,i_m}$, which are given by linear algebraic equations with N unknows. Once with the head terms, the first two moments of head can be obtained with simple algebraic operations. Because the structure of the head term Eqs. (40)–(43) is the same as that of the moment equations for $C_{Yh}(\mathbf{x};\chi,\tau)$ and $C_h(\mathbf{x},t;\chi,\tau)$ (e.g., (4.13)–(4.14) of [30]), the computational effort for solving for $h^{(m)}_{i_1,i_2,\ldots,i_m}(\mathbf{x},t)$ on a grid of N nodes is more or less the same as that for $C_h(\mathbf{x},t;\chi,\tau)$, or $C_{Yh}(\mathbf{x};\chi,\tau)$, for each reference point (χ,τ). Hence, the effectiveness of KL-based approach largely depends on the number of times required to solve these linear algebraic equations. Due to symmetry, to obtain $h^{(m)}_{i_i,i_2,\ldots,i_m}$, where $i_j=\overline{1,n}$, the number of times required to solve linear algebraic equation with N unknows is $S_m=n(n+1)\cdots(n+m-1)/m!$. For example, for $n=20$, we need to solve (30)–(33) for $h^{(2)}_{ij}$ for $S_2=210$ times.

Two important factors contribute to the efficiency of this KL-based moment-equation (KLME) approach, as shown numerically in the next section. First, the overall magnitudes of $h^{(m)}_{i_i,i_2,\ldots,i_m}$ decrease with order m. This allows us to use a relatively low order approximation for small to moderate variability σ^2_Y. In addition, for a fixed m, the magnitudes of $h^{(m)}_{i_i,i_2,\ldots,i_m}$ quickly approach zero (statistically) as indices increase, which means that we can approximate $h^{(m)}$ with a relative small number of terms. For the case of a grid of 41×41 mesh (i.e., 1681 nodes) as in our examples in the next section, up to first-order, the conventional moment equation approach requires to solve the moment equations on the grid for $2N=3362$ times while the KL-based approach only needs to solve the head term equations for a few hundreds times on the same grid. Therefore, for a moderate problem size (say, $N\geqslant 400$), the KL-based perturbation approach may be much more efficient than the conventional perturbation approach. The relative efficiency of the KL-based approach improves as the domain size increases.

The computational efforts of the KL-based approach can be reduced significantly if we take advantage of the orthogonal Gaussian random variables $\{\xi_n\}$. For example, in computing second moment terms (e.g., head variance) up to third-order in σ^2_Y, terms $h^{(5)}_{jklmn}$ and $h^{(1)}_i$ always appear together as the coefficient of term $\langle\xi_i\xi_j\xi_k\xi_l\xi_m\xi_n\rangle$. As a result, if the set of indices $\{jklmn\}$ has more than one odd number of occurrences, the term $h^{(5)}_{jklmn}$ does not need to be solved because $\langle\xi_i\xi_j\xi_k\xi_l\xi_m\xi_n\rangle\equiv 0$. For instance, the term $h^{(5)}_{1,3,4,4,5}$ can be skipped because the set $\{1,3,4,4,5\}$ has three indices that have odd number of occurrences. The contribution of $h^{(5)}_{1,3,4,4,5}$ to head variance must be zero because $\langle\xi_i\xi_1\xi_3\xi^2_4\xi_5\rangle\equiv 0$, no matter what the index i is.

The deterministic coefficients $h^{(m)}_{i_i,i_2,\ldots,i_m}$ can be solved using either finite element or finite difference method, which yields sets of linear algebraic equations in a form of $\mathbf{Ax}=\mathbf{b}$. It should be noted that the coefficient matrix $\mathbf{A}$ is always the same for all those equations for $h^{(m)}_{i_i,i_2,\ldots,i_m}$.

6. Illustrative examples

In this section, we attempt to examine the validity of the proposed KLME approach in computing higher-order head moments for flow in hypothetical saturated porous media, by comparing model results with those from Monte Carlo simulations.

We consider a two-dimensional domain in a saturated heterogeneous porous medium. The flow domain is a square of a size $L_1=L_2=10$ $[L]$ (where L is any consistent length unit), uniformly discretized into 40×40 square elements. The non-flow conditions are prescribed at two lateral boundaries. The hydraulic head is prescribed at the left and right boundaries as 10.5 $[L]$ and 10.0 $[L]$, respectively, which produces a mean flow from the left to the right. The mean of the log hydraulic conductivity is given as $\langle Y\rangle=0.0$ (i.e., the geometric mean saturated hydraulic conductivity $K_G=1.0$ $[L/T]$, where T is any consistent time unit).

For simplicity, it is assumed in the following examples that the log saturated hydraulic conductivity $Y(\mathbf{x})=\ln K_s(\mathbf{x})$ is second-order stationary with a separable exponential covariance function

$$C_Y(\mathbf{x},\mathbf{y})=C_Y(x_1,x_2;y_1,y_2)=\sigma^2_Y\exp\left[-\frac{|x_1-y_1|}{\eta}-\frac{|x_2-y_2|}{\eta}\right], \tag{50}$$

where η is the correlation scale. In this case, eigenvalues λ_n, $n = 1, 2, \ldots$, and their corresponding eigenfunctions f_n, $n = 1, 2, \ldots$, can be determined analytically by first solving Eq. (12) for w and computing λ based on (10), and then combining eigenvalues and eigenfunctions from each dimension using (13) and (14).

The eigenvalues are monotonically nonincreasing as illustrated in Fig. 1(a) for case 1 to case 3 with different correlation lengths. Note that the product of two monotonically decreasing series may not be monotonically decreasing. Fig. 1(b) shows the sum of eigenvalues as a function of terms included. The figure indicates that for the case with a large correlation length, only a few terms are required to approximate Y' defined in Eq. (8), while for a relatively small correlation length, a larger number of terms are needed to approximate Y' with a reasonable accuracy. Some of the eigenfunctions for case 2 are depicted in Fig. 2. Any realization of log hydraulic conductivity is a summation of an infinite number of such eigenfunctions f_n weighted by the product of $\sqrt{\lambda_n}$ and an independently generated Gaussian random variable ξ_n. The terms in series (8) not only statistically decrease in magnitude (the nth term has a zero mean and a variance of $\lambda_n f_n^2(\mathbf{x})$ whose average over domain D is λ_n that decreases with the increase of n) but also reduce in scale. By approximating Y' as a summation of a finite number rather than an infinite number of terms, one in fact ignores the small-scale variation of log hydraulic conductivity.

To investigate the applicability of the proposed KLME approach, we designed a series of numerical runs with different correlation lengths η and various degrees of spatial variability σ_Y^2. Cases 1–3 aim to investigate the effects of correlation lengths ($\eta = 1$, 4, and 10, respectively) on the KLME approach. In these cases, the degree of spatial variability is kept at $\sigma_Y^2 = 1.0$, corresponding to $CV = 131\%$ where CV is the coefficient of variation of hydraulic conductivity. Cases 4–6 are compared against case 2 to examine the impact of log hydraulic conductivity variability ($\sigma_Y^2 = 0.25$, 2.0, and 4.0, respectively, which correspond to $CV = 53\%$, 253%, and 732%). The number of terms included in approximating $h^{(m)}_{i_1,i_2,\ldots,i_m}$ for all cases are 100, 40, 30, 20, and 10 for $m = 1$, 2, 3, 4, and 5, respectively, except for case 1 in which the number of terms in approximating $h^{(1)}_n$ is 500 instead of 100. It should be noted that, for the purpose of comparison, we have included sufficiently large numbers of terms in these approximations. The effect of the numbers of terms retained in approximations will be discussed later.

For the purpose of comparison, we conducted Monte Carlo simulations. For each case, we use 5000 two-dimensional unconditional realizations generated on the grid of 41×41 nodes with the separable covariance function given in (50), based on (8) with 200 terms. The quality of these realizations are examined for each case by comparing their sample statistics (mean, variance, and correlation length) of these realizations with the specified mean and covariance functions. The comparisons show that the generated random fields reproduce the specified mean and covariance functions very well. The steady state, saturated flow equation is solved for each realization of the log hydraulic conductivity, using finite-element heat- and mass-transfer code (FEHM) developed by Zyvoloski et al. [33]. Then, the sample statistics of the flow field, i.e., the mean prediction of head

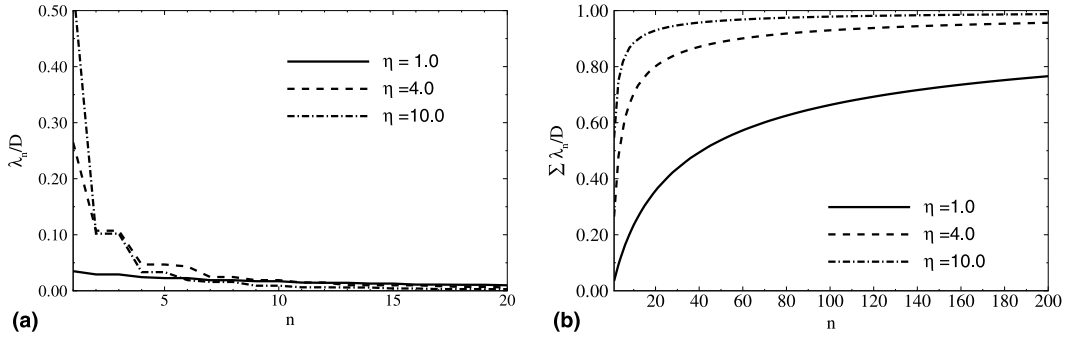

Fig. 1. Series of eigenvalues and their finite sums for two-dimensional square flow domain with a separable covariance function of correlation length: (a) $\eta = 1.0$; (b) $\eta = 4.0$; and (c) $\eta = 10.0$.

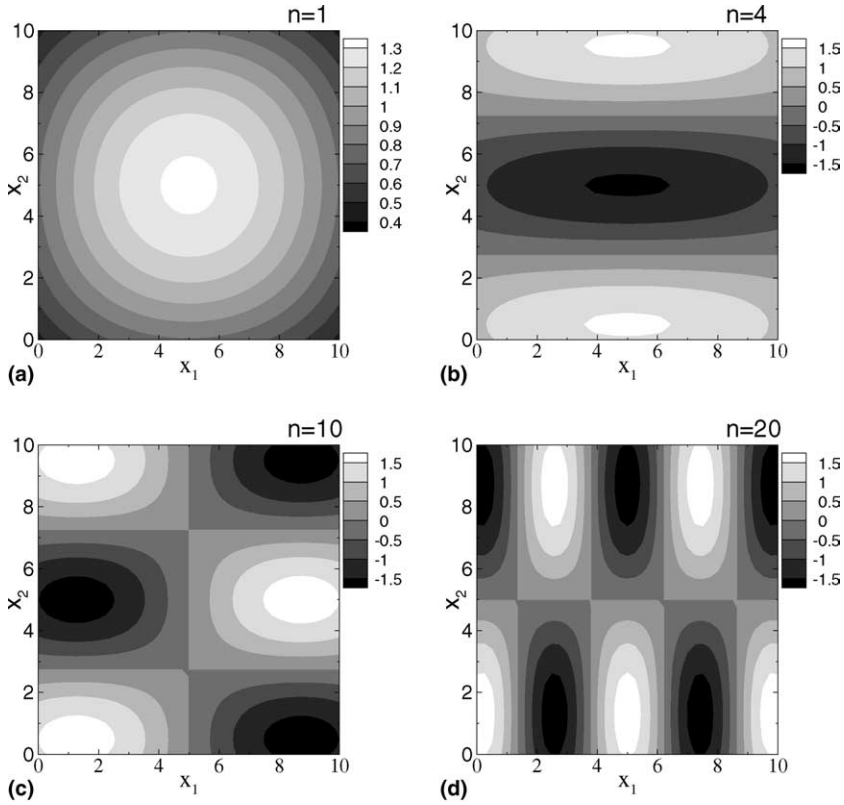

Fig. 2. Examples of eigenfunctions f_n for case 1: (a) f_1; (b) f_4; (c) f_{10}; and (d) f_{20}.

as well as its associated uncertainty (variance), are computed from the realizations. These statistics are considered the "true" solutions that are used to compare against the proposed higher-order KLME approach.

We also compared the results from the KLME approach against those from the conventional first-order moment-equation-based approach (CME), as developed by Zhang and Lu [31]. Here the covariance function of log hydraulic conductivity used in this study is in a separable form, i.e., (50), rather than exponential form as in [31]. It is expected that, while the higher-order approximations of head variance from the KLME approach should be close to Monte Carlo results, their first-order approximations shall be almost identical to those from the conventional moment-equation-based approach, if n_1, the number of terms included in $h^{(1)}$ of (23), is sufficiently large. That is to say, the closeness of the first-order variances derived from the conventional moment-equation-based approach and from the KLME approach is an indicator showing if n_1 is large enough.

7. Results and discussions

7.1. Effect of the correlation length η

Due to the particular boundary configurations in our examples, the mean head computed from different approaches do not have significant difference and therefore will not be discussed. Here we focus our

discussion only on head variance. We should mention here that in the following discussion, the order of approximations for head variance is in terms of σ_Y^2.

Fig. 3 compares the head variance from Monte Carlo simulations, the CME approach, and the KLME approach up to third-order in σ_Y^2, for different correlation lengths. Fig. 3(a) indicates that, for the case with a small correlation length, both the first-order CME approach and the first-order KLME approach yield almost identical head variance as the Monte Carlo simulations, even though the spatial variability is as large as $\sigma_Y^2 = 1.0$, indicating that 500 terms are sufficient to approximate $h^{(1)}(\mathbf{x})$ in (23). The computational effort for solving each term in the $h_n^{(1)}(\mathbf{x})$ series of (25) is equivalent to that for $C_{Yh}(\mathbf{x}, \mathbf{y})$ for each reference point $\mathbf{y}$, and the derivation of the (first-order) covariances C_{Yh} and C_h from $h_n^{(1)}(\mathbf{x})$ involves only simple algebraic operations. As mentioned before, it requires to solve the $C_{Yh}(\mathbf{x}, \mathbf{y})$ and $C_h(\mathbf{x}, \mathbf{y})$ equations about $2N$ times in the conventional moment-equation-based approach (in this case, $N = 1681$). Therefore, for this case the KL-based approach is computationally more efficient than the conventional moment-equation-based approach.

In addition, for relatively large correlation lengths, the first-order approximations (for both CME and KLME) of head variance deviate from Monte Carlo results. To predict head variance more accurately, higher-order approximations are required. Fig. 3(b) and (c) show that second-order (in σ_Y^2) approximations are very close to Monte Carlo results, though third-order (in σ_Y^2) approximations are better and almost identical to Monte Carlo results. Note that solving first-order head variance for case 2 and 3 using the KLME approach, it requires only 100 times to solve sets of linear algebraic equations of N unknows, compared to $2N$ ($= 3362$) times for the first-order CME approach.

As shown in Fig. 1, the number of terms needed to be retained in the expansions increases with the decreases of the correlation length η. When the ratio of the correlation length to the domain size (η') is small which is very likely the case for simulating large-scale problems, first-order approximations may be accurate enough (for a moderate variability σ_Y^2) as the higher-order terms are found to be negligible. Thus, such a case can still be handled efficiently with the first-order KLME approach. With the increase of η', as ex-

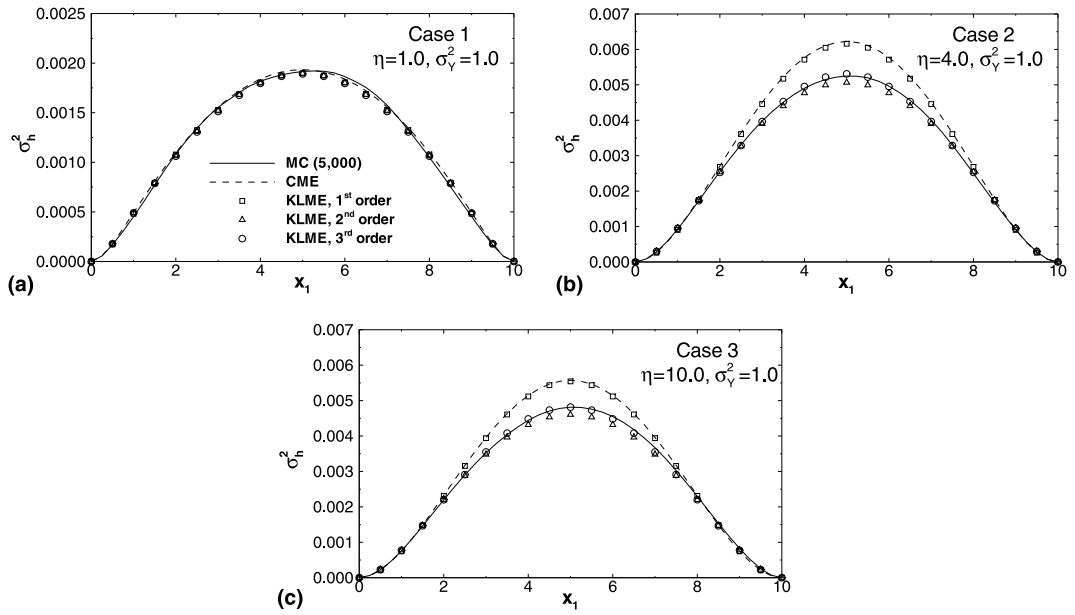

Fig. 3. Comparisons of head variance (along the cross-section $x_2 = 5.0$) derived from MC, CME, and KLME up to third-order in σ_Y^2, for cases with correlation length: (a) $\eta = 1.0$; (b) $\eta = 4.0$; and (c) $\eta = 10.0$.

plained later in Fig. 8 the higher-order corrections become important while the number of terms required to retain in the expansions decreases.

7.2. Effect of spatial variability σ_Y^2

To explore the effect of spatial variability σ_Y^2 on validity of the proposed KL-based moment approach, we examined three more cases (cases 4, 5, and 6), together with case 2, with the same correlation length ($\eta = 4.0$) but various degrees of spatial variability ($\sigma_Y^2 = 0.25$, 1.0, 2.0, and 4.0). Comparisons of the head variance derived from Monte Carlo simulations, the first-order CME approach, and the KLME approach up to third-order in σ_Y^2 are illustrated in Fig. 4. As expected, when σ_Y^2 is small (Fig. 4(a)), head variance obtained from different approaches do not have significant differences. For all cases, the first-order (in σ_Y^2) head variance from the CME approach is the same as the first-order solution from the KLME approach for all four cases examined, simply implying that the number of terms ($n_1 = 100$) included in $h^{(1)}$ are adequate to approximate $h^{(1)}$. Comparing to the first-order CME approach, with the increase of σ_Y^2, the advantage of the KLME approach is obvious. At $\sigma_Y^2 = 1.0$, the estimation error of head variance (at the center of the domain) introduced by the first-order CME approach (and also the first-order KLME approach) is 17.3%, while the estimation error is 3.4% for the second-order solution of the KLME approach and 1.1% for the third-order solution of the KLME approach. At $\sigma_Y^2 = 2.0$, the estimation error of head variance for the first-order solutions is 33.6%, while they are 14.4% and 6.6%, respectively, for the second-order and the third-order solutions of the KLME approach.

When the porous media are strongly heterogeneous (case 6, $\sigma_Y^2 = 4.0$), though higher-order corrections of the KLME approach make some improvement on estimating head variance over the first-order solution of the CME approach, the variance still deviates greatly from that from Monte Carlo simulations, as shown in Fig. 4(c). We tried to increase the numbers of terms included in $h^{(i)}(\mathbf{x}, t)$, $i = \overline{1,5}$, and found that this does

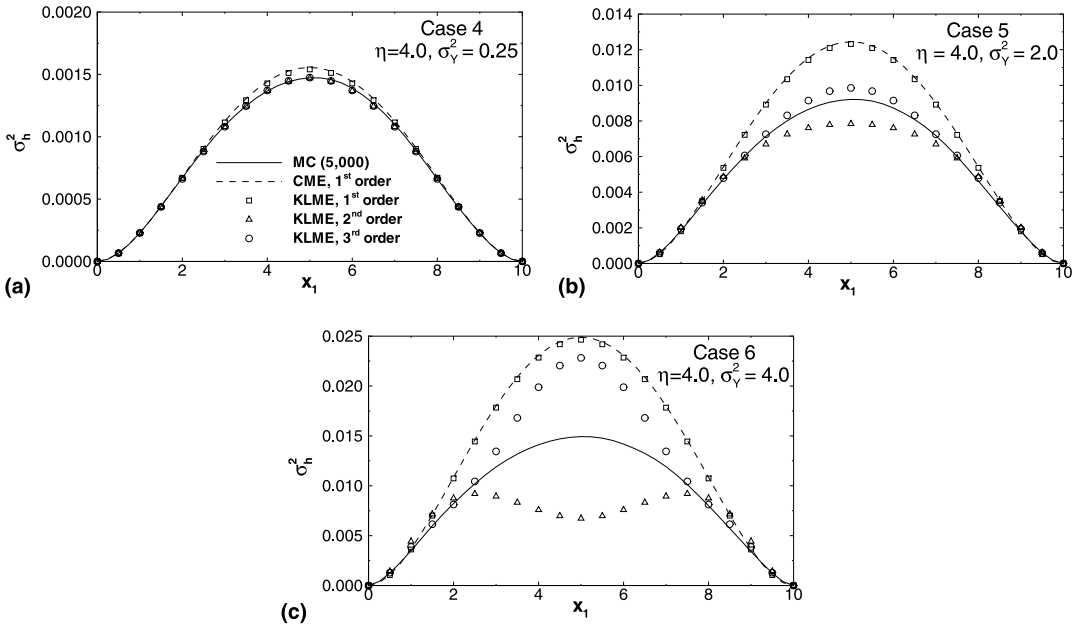

Fig. 4. Comparisons of head variance (along the cross-section $x_2 = 5.0$) derived from MC, CME, and KLME up to third-order in σ_Y^2, for the cases with: (a) $\sigma_Y^2 = 0.25$; (b) $\sigma_Y^2 = 2.0$; and (c) $\sigma_Y^2 = 4.0$.

not make a significant improvement. We suspect that for such highly heterogeneous porous media, we may need to include terms of even higher order in Eq. (44). For example, to compute head variance up to fourth-order in σ_Y^2, we have to include up to seventh-order terms in (44). The slow convergence is further discussed later with Fig. 9.

7.3. Effect of the number of terms in expansions

The advantage of the proposed KL-based moment approach largely depends on how many terms are required to approximate $h^{(m)}_{i_1,i_2,\ldots,i_m}$. In the examples shown above, for the purpose of comparison, we included relatively large numbers of terms in these approximations. However, the numbers of terms included in these approximations can be much less. Here we take case 2 as an example. Fig. 5 depicts the values of $h^{(m)}_{i_1,i_2,\ldots,i_m}$ at the center of the domain for various orders m and indices. It is seen that the magnitude of $h^{(m)}$ decreases with m. For example, the maximum absolute value of $h^{(1)}_i$ is about one order larger than that of $h^{(2)}_{ij}$, and the maximum absolute value of $h^{(3)}_{ijk}$ is about one order larger than that of $h^{(4)}_{ijkl}$. Furthermore, for a fixed m, the magnitude of $h^{(m)}_{i_1,i_2,\ldots,i_m}$ decreases statistically as the increase of indices. This allows us to take only small numbers of terms in approximating $h^{(m)}$.

We reduce the numbers of terms included in approximating $h^{(1)}_i$, $h^{(2)}_{ij}$, $h^{(3)}_{ijk}$, $h^{(4)}_{ijkl}$, and $h^{(5)}_{ijklm}$ to 100, 10, 10, 5, and 5, respectively, i.e., index i in $h^{(1)}_i$ running up to 100 and each index in $h^{(2)}_{ij}$ running up to 10, and so on. For instance, Eqs. (25)–(28) need to be solved for 100 times, and Eqs. (30)–(33) need to be solved for 55 times (noting that $h^{(2)}_{ij}$ is symmetric with respect to indices i and j). The total number of times to solve similar equations to obtain $h^{(1)}_i$, $h^{(2)}_{ij}$, $h^{(3)}_{ijk}$, $h^{(4)}_{ijkl}$, and $h^{(5)}_{ijklm}$ will be $100 + 55 + 220 + 70 + 75 = 520$, which is much less than the number of Monte Carlo simulations (at the order of few thousands) required at $\sigma_Y^2 = 1.0$ and also less than the number of times for solving the $C_{Yh}(\mathbf{x}, \mathbf{y})$ and $C_h(\mathbf{x}, \mathbf{y})$ covariance equations

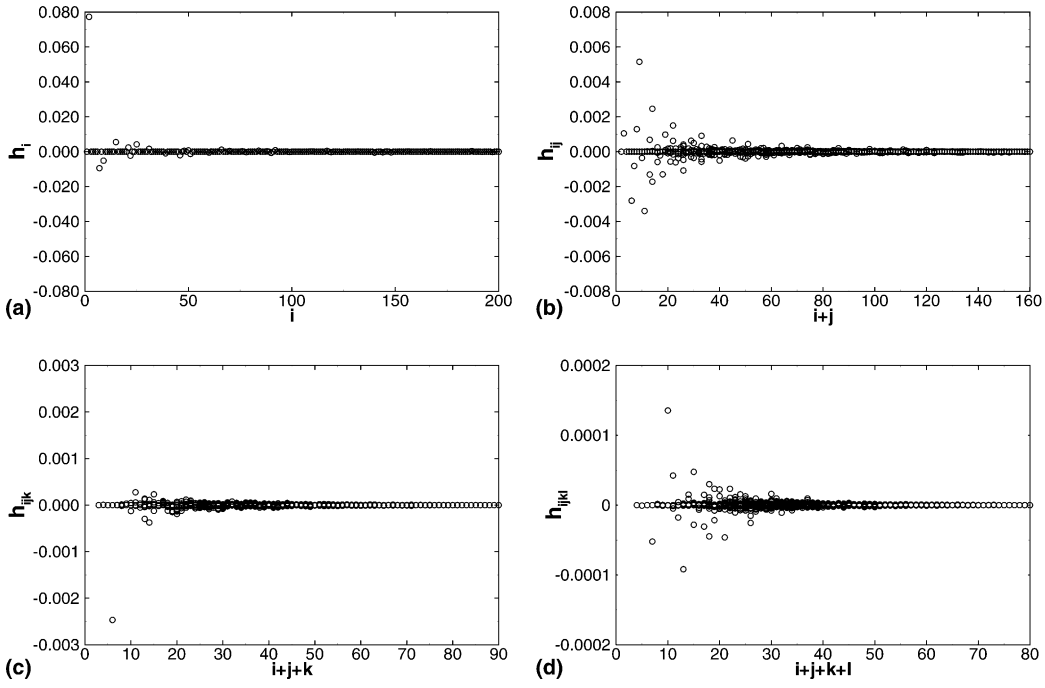

Fig. 5. Values of $h^{(m)}_{i_1,i_2,\ldots,i_m}$ at the center of the domain for case 2 (a) $h^{(1)}_i$; (b) $h^{(2)}_{ij}$; (c) $h^{(3)}_{ijk}$; and (d) $h^{(4)}_{ijkl}$.

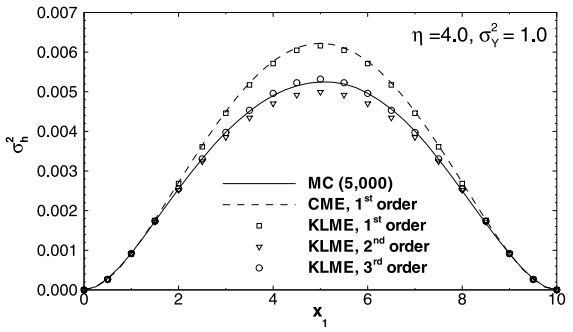

Fig. 6. Comparisons of σ_h^2 (along the cross-section $x_2 = 5.0$) derived from MC, CME, and KLME to third-order in σ_Y^2 for case 2 with 100, 10, 10, 5, and 5 terms in approximating $h^{(1)}$, $h^{(2)}$, $h^{(3)}$, $h^{(4)}$, and $h^{(5)}$, respectively.

($2N = 3362$, in this case) in the first-order CME approach. We have to emphasize that the total computational requirement for solving up to third-order approximation using the KLME approach is still less than that required by the first-order CME approach.

Fig. 6 shows the head variance at different order of approximations, for case 2, computed using reduced numbers of terms in approximating $h_i^{(1)}$, $h_{ij}^{(2)}$, $h_{ijk}^{(3)}$, $h_{ijkl}^{(4)}$, and $h_{ijklm}^{(5)}$. Compared to Fig. 3(b) where the respective terms are 100, 40, 30, 20, and 10, it is seen that the behaviors observed with reduced numbers of terms are almost the same as in Fig. 3(b). For this case, higher-order approximations with only a few leading terms capture most of the variability of head variance.

As mentioned earlier, when the correlation length is relatively small, the number of terms, n_1, required to approximate $h^{(1)}(\mathbf{x}, t)$ in (23) should be large. To investigate how the accuracy of estimations depending on n_1, we ran a few more cases in which all parameters are the same as in case 1 but with a decreasing number of terms $n_1 = 100$ and $n_1 = 200$, as compared with $n_1 = 500$ in case 1 ($\eta = 1.0$). The head variance computed using different numbers of terms n_1 is illustrated in Fig. 7. The figure indicates that 100 terms are enough to approximate $h^{(1)}(\mathbf{x}, t)$ in (23) for this case. This can also be seen from Fig. 8, where values of $h_{i_1,i_2,\ldots,i_m}^{(m)}$ at the center of the domain are plotted against their indices. Fig. 8 also explains why high-order terms do not have significant contributions to head variance as shown in Fig. 3(a). Although at each order they decay at a slower rate, the higher-order coefficients $h_{i_1,i_2,\ldots,i_m}^{(m)}$ for case 1 are much smaller than their counterparts presented in Fig. 5 for case 2 ($\eta = 4.0$).

When the correlation scale η is fixed (relative to the domain szie), the patterns of the head coefficient terms $h_{i_1,i_2,\ldots,i_m}^{(m)}$ do not change at each order regardless of σ_Y. Fig. 9 shows the values of $h_{i_1,i_2,\ldots,i_m}^{(m)}$ at the center

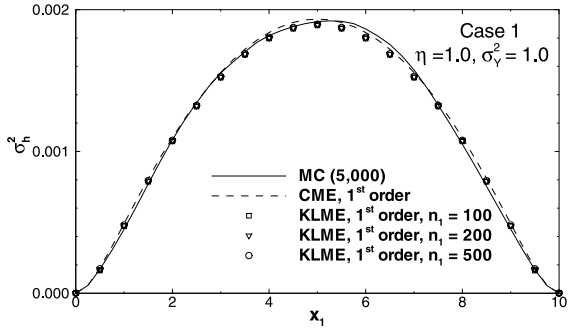

Fig. 7. Comparisons of head variance σ_h^2 (along the cross-section $x_2 = 5.0$) for case 1 derived from MC, the first-order CME, and the first-order KLME with 200, 500, and 1000 terms in approximating $h^{(1)}$ in (23).

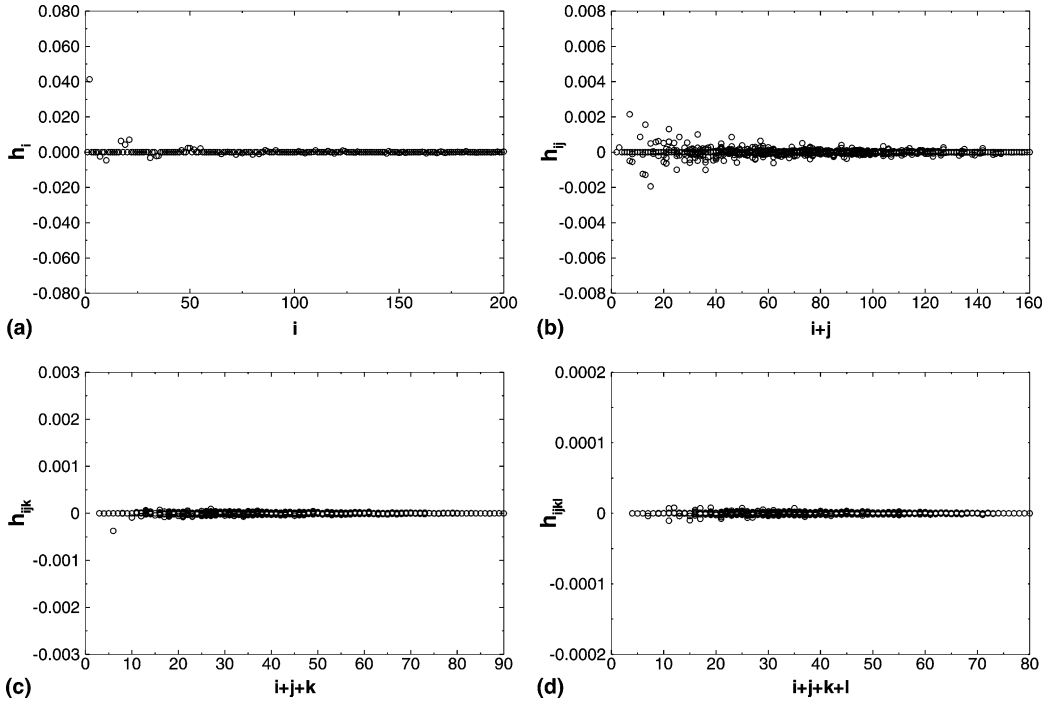

Fig. 8. Values of $h^{(m)}_{i_1,i_2,\ldots,i_m}$ at the center of the domain for case 1: (a) $h^{(1)}_i$; (b) $h^{(2)}_{ij}$; (c) $h^{(3)}_{ijk}$; and (d) $h^{(4)}_{ijkl}$.

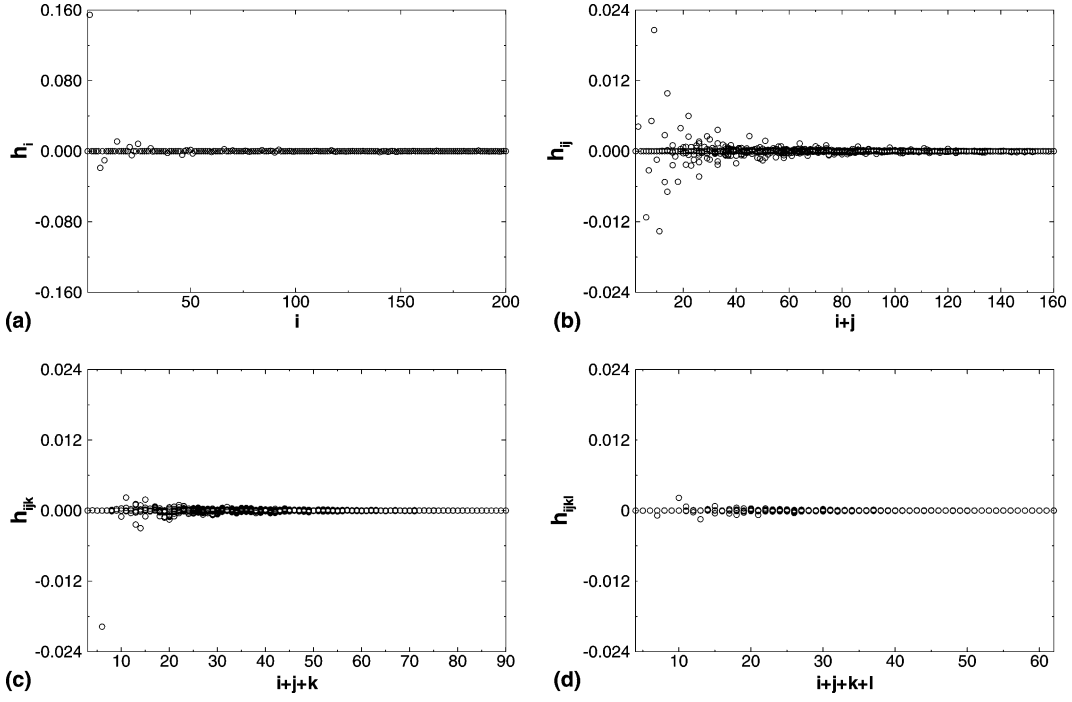

Fig. 9. Values of $h^{(m)}_{i_1,i_2,\ldots,i_m}$ at the center of the domain for case 6: (a) $h^{(1)}_i$; (b) $h^{(2)}_{ij}$; (c) $h^{(3)}_{ijk}$; and (d) $h^{(4)}_{ijkl}$.

of the domain for various orders m and indices for case 6 where $\eta = 4$ and $\sigma_Y = 2$. Fig. 9 can be obtained from Fig. 5 via rescaling $h_i^{(1)}$, $h_{ij}^{(2)}$, $h_{ijk}^{(3)}$, and $h_{ijkl}^{(4)}$, respectively, by 2, 4, 8, and 16. Although at each order the patterns are exactly the same as those in Fig. 5, the relative magnitudes for various orders are significantly different in Fig. 9. The second-order coefficients $h_{ij}^{(2)}$ are still approximately one order of magnitude smaller than the first-order counterparts $h_i^{(1)}$. However, the third-order coefficients $h_{ijk}^{(3)}$ are at the same order as $h_{ij}^{(2)}$. Likewise, the fourth-order coefficients $h_{ijkl}^{(4)}$ are not much smaller than $h_{ijk}^{(3)}$. This explains the slow convergence observed in Fig. 4(c) for case 6. It is fully expected that a further increase of σ_Y may lead to divergence. Future studies shall pinpoint the exact validity range of the proposed approach and explore the possibility of developing more efficient expansions for handling extremely large variabilities.

8. Summary and conclusions

In this study, we combined the moment-equation approach with the Karhunen–Loève and polynomial expansions to evaluate higher-order moments for saturated flow in randomly heterogeneous porous media. We first decomposed the log hydraulic conductivity into an infinite series related to eigenvalues and eigenfunctions of the covariance function of log hydraulic conductivity as well as a set of standard Gaussian random variables. By assuming that the covariance function C_Y is separable and that the simulation domain is rectangular in two-dimensional cases or brick-shaped in three-dimensional cases, the eigenvalues and eigenfunctions can be derived analytically. In general, however, for other covariance functions the eigenvalues and eigenfunctions have to be solved numerically. We then decomposed the head into a series whose terms $h^{(n)}$ are nth order in terms of σ_Y. By further assuming that $h^{(n)}$ can be expanded into a series in terms of the product of n Gaussian random variables used in expanding Y, we arrived at sets of equations for determining the deterministic coefficients in these expansions. Unlike in the polynomial chaos expansion approach of Ghanem and Spanos [8] or the generalized polynomial chaos expansion of Xiu and Karniadakis [28] where all the equations governing the coefficients are coupled, the equations from the present approach are recursive in that the high-order equations depend on the lower-order ones but not vice versa. In addition, in the present approach the order of approximation is clear for each term in terms of σ_Y whereas in those of [8,28] the level of approximation is mixed in each term of the expansions with respect to σ_Y.

Once the coefficients are solved, the mean head and head covariance can be computed directly without solving additional equations. The moment-equation approach based on Karhunen–Loève decomposition (KLME) allows us to evaluate mean head up to fourth-order in σ_Y and head covariance up to third-order in σ_Y^2. We demonstrated the KLME approach with some examples of steady state saturated flow in a two-dimensional rectangular domain and compared our results with those from Monte Carlo simulations and from the conventional first-order moment-equation based approach. This study leads to the following major conclusions:

1. The moment-equation approach based on Karhunen–Loève decomposition (KLME) makes it possible to evaluate higher-order flow moments with relatively small computational efforts.
2. To first-order in the variance of log hydraulic conductivity (i.e., σ_Y^2), the KLME approach gives results that are consistent with those by the CME approach. Owing to the rapid convergence of the first-order head term expansion (23), the first-order KLME approach is generally much more efficient than the CME approach for the cases considered in this study under a wide range of correlation lengths and variability levels.
3. In general, the agreement between the KLME and Monte Carlo simulation results improves with the decrease of σ_Y^2, with the reduction of the correlation scale (i.e., η) relative to the domain size, and with the increase of the order in the KLME approximations. For $\sigma_Y^2 = 1$ and $\eta = 1$, even the first-order KLME approximation gives very accurate results for the head moments. For $\eta = 4$ and 10, the KLME

approach give results closer to those by Monte Carlo simulations when higher-order terms are included. The third-order KLME approximation is accurate and efficient at least for σ_Y^2 as large as 2.0 (corresponding to the coefficient of variation being 253%) and η as large as 4.0. Our examples reveal that the KLME approach is generally more efficient computationally than the Monte Carlo method.

4. The efficiency of the KL-based moment method depends on the ratio of the correlation length to the domain size. Small correlation length requires more terms in expansions of $h^{(n)}$ and thus requires more computational efforts. However, it seems that, when the ratio is small, first-order approximations is accurate enough and thus the computational costs for the KLME approach is still much less than that required for the CME approach.

Appendix A

To find eigenvalues and eigenfunctions for a one-dimensional stochastic process with an exponential covariance $C_Y(x_1, y_1) = \sigma_Y^2 \exp(-|x_1 - y_1|/\eta)$, where σ_Y^2 and η are the variance and correlation length of the process, respectively, from definition, one has

$$\lambda f(x_1) = \sigma_Y^2 \int_D \mathrm{e}^{-|x_1-y_1|/\eta} f(y_1)\mathrm{d}y_1. \tag{A.1}$$

Taking derivative of (A.1) with respect to x_1 yields

$$\frac{\lambda}{\sigma_Y^2} f'(x_1) = -\frac{1}{\eta}\int_0^{x_1} \mathrm{e}^{(y_1-x_1)/\eta} f(y_1)\mathrm{d}y_1 + \frac{1}{\eta}\int_{x_1}^{L} \mathrm{e}^{(x_1-y_1)/\eta} f(y_1)\mathrm{d}y_1. \tag{A.2}$$

Taking derivative again gives an equation for eigenfunction $f(x)$:

$$f''(x_1) + \frac{2\eta\sigma_Y^2 - \lambda}{\lambda\eta^2} f(x_1) = 0. \tag{A.3}$$

The boundary conditions associated with (A.3) can be determined from (A.2) by letting $x_1 = 0$ and $x_1 = L$:

$$\eta f'(0) = f(0), \quad \eta f'(L) = -f(L). \tag{A.4}$$

The general solution of Eq. (A.3) is

$$f(x) = a\cos(wx) + b\sin(wx), \tag{A.5}$$

where $w^2 = (2\eta\sigma_Y^2 - \lambda)/(\lambda\eta^2)$. By using two boundary conditions in (A.4), one obtains two linear equations for determining coefficients a and b in (A.5).

$$\begin{aligned} &a - \eta w b = 0, \\ &[-w\eta\sin(wL) + \cos(wL)]a + [w\eta\cos(wL) + \sin(wL)]b = 0. \end{aligned} \tag{A.6}$$

Limiting to nontrivial solutions of (A.6) yields an equation for w,

$$(\eta^2 w^2 - 1)\sin(wL) = 2\eta w\cos(wL), \tag{A.7}$$

which is (12). For given η and L, we can solve w from (A.7), which yields a series of (positive) w_n, $n = 1, 2, \ldots$. The eigenvalue corresponding to w_n can be found from the definition of w:

$$\lambda_n = \frac{2\eta\sigma_Y^2}{\eta^2 w_n^2 + 1}. \tag{A.8}$$

Certainly, different w_n gives different coefficients a and b in Eq. (A.5), thus the eigenfunction associated with w_n or λ_n is

$$f_n(x) = a_n \cos(w_n x) + b_n \sin(w_n x), \tag{A.9}$$

where the coefficients a_n and b_n can be determined by the condition that eigenfunctions are normalized, i.e, $\int_D f_n^2(x) = 1$. The latter leads to

$$\begin{aligned} b_n &= \frac{1}{\sqrt{(\eta^2 w_n^2 + 1)L/2 + \eta}}, \\ a_n &= \eta w_n b_n. \end{aligned} \tag{A.10}$$

Note that while eigenvalues λ_n are proportional to σ_Y^2, the eigenfunctions $f_n(\mathbf{x})$ are independent of σ_Y^2 and depend only on the domain size L and the correlation length η.

For a large domain size, solving (A.7) may be problematic. The equation can be solved more easily by using dimensionless formulation. Let $x' = x/L$, $w' = wL$, and $\eta' = \eta/L$, (A.7) becomes

$$(\eta'^2 w'^2 - 1)\sin(w') = 2\eta' w' \cos(w'), \tag{A.11}$$

Note that w' depends only on η', the ratio of the correlation length to the domain size. It can be shown that the corresponding terms $\lambda_n' = \lambda_n/L$, $a_n' = a_n\sqrt{L}$, $b_n' = b_n\sqrt{L}$, and $f_n'(x) = f_n\sqrt{L}$. This leads to $\sqrt{\lambda_n} f_n(x) \equiv \sqrt{\lambda_n'} f_n'(x')$. Because $\sqrt{\lambda_n}$ and $f_n(x)$ appear always together in derivation of the KL-based moment equations, we can directly use λ_n' and $f_n'(x')$ derived from solving (A.11), without transforming them back to the original space. One of the advantages of the dimensionless formulation is that the structures of eigenfunctions depend only on the ratio of the correlation length to the domain size, and are independent of the actual domain size.

We should emphasize here that we only need to solve one characteristic equation, i.e., (A.7), while in literature [9] w_n are solved from the following two characteristic equations:

$$w\eta \tan(wL) - 1 = 0, \tag{A.12}$$

$$w\eta + \tan(wL) = 0, \tag{A.13}$$

respectively, and then taking w_n from the first equation for even n or from the second equation for odd n. Similarly, both eigenvalues λ_n and their eigenfunctions $f_n(x)$ are chosen from those corresponding to these two characteristic equations for even or odd n. Certainly, our approach saves computational effort and reduces complexity.

As a matter of fact, (A.12) and (A.13) can be combined into (A.7). It can be shown that roots of Eqs. (A.12) and (A.13) do not overlap, thus combining (A.12) and (A.13) into (A.7) will not lose any roots.

References

[1] O. Amir, S.P. Neuman, Gaussian closure of one-dimensional unsaturated flow in randomly heterogeneous soils, Transp. Porous Media 44 (2001) 355.
[2] R. Courant, D. Hilbert, Methods of Mathematical Physics, Interscience, New York, 1953.
[3] J.H. Cushman, The Physics of Fluids in Hierarchical Porous Media: Angstroms to Miles, Kluwer Academic Publishers, Norwell, MA, 1997.
[4] G. Dagan, Stochastic modeling of groundwater flow by unconditional and conditional probabilities: 1. Conditional simulation and the direct problem, Water Resour. Res. 18 (1982) 813.
[5] G. Dagan, Flow and Transport in Porous Formations, Springer, New York, 1989.
[6] L.W. Gelhar, Stochastic Subsurface Hydrology, Prentice-Hall, Englewood Cliffs, NJ, 1993.

[7] L.W. Gelhar, C.L. Axness, Three-dimensional stochastic analysis of macrodispersion in aquifers, Water Resour. Res. 19 (1983) 161.
[8] R. Ghanem, P.D. Spanos, Stochastic Finite Elements: A Spectral Approach, Springer, New York, 1991.
[9] R. Ghanem, R.M. Kruger, Numerical solution of spectral stochastic finite element systems, Comput. Methods Appl. Mech. Eng. 129 (1996) 289.
[10] R. Ghanem, Scale of fluctuation and the propagation of uncertainty in random porous media, Water Resour. Res. 34 (1998) 2123.
[11] R. Ghanem, Probabilistic characterization of transport in heterogeneous media, Comput. Methods Appl. Mech. Eng. 158 (1998) 199.
[12] R. Ghanem, S. Dham, Stochastic finite element analysis for multiphase flow in heterogeneous porous media, Transp. Porous Media 32 (1998) 239.
[13] R. Ghanem, Ingredients for a general purpose stochastic finite elements implementation, Comput. Methods Appl. Mech. Eng. 168 (1999) 19.
[14] W.D. Graham, D. McLaughlin, Stochastic analysis of nonstationary subsurface solute transport, 1. Unconditional moments, Water Resour. Res. 25 (1989) 215.
[15] A. Guadagnini, S.P. Neuman, Nonlocal and localized analyses of conditional mean steady state flow in bounded, randomly nonuniform domains: 1. Theory and computational approach, Water Resour. Res. 35 (1999) 2999.
[16] K.C. Hsu, D. Zhang, S.P. Neuman, Higher-order effects on flow and transport in randomly heterogeneous porous media, Water Resour. Res. 32 (1996) 571.
[17] P. Indelman, Averaging of unsteady flows in heterogeneous media of stationary conductivity, J. Fluid Mech. 310 (1996) 39.
[18] L. Li, H.A. Tchelepi, D. Zhang, Perturbation-based moment equation approach for flow in heterogeneous porous media: Applicability range and analysis of high-order terms, J. Comput. Phys. 188 (2003) 296.
[19] M. Loeve, Probability Theory, fourth ed., Springer, Berlin, 1977.
[20] Z. Lu, S.P. Neuman, A. Guadagnini, D.M. Tartakovsky, Conditional moment analysis of steady state unsaturated flow in bounded randomly heterogeneous soils, Water Resour. Res. 38 (2002), 10.1029/2001WR000278.
[21] S.P. Neuman, C.L. Winter, C.M. Newman, Stochastic theory of field-scale Fickian dispersion in anisotropic porous media, Water Resour. Res. 23 (1987) 453.
[22] S.P. Neuman, Eulerian–Lagrangian theory of transport in space–time nonstationary velocity fields: Exact nonlocal formalism by conditional moments and weak approximations, Water Resour. Res. 29 (1993) 633.
[23] R.V. Roy, S.T. Grilli, Probabilistic analysis of the flow in random porous media by stochastic boundary elements, Eng. Anal. Boundary Elements 19 (1997) 239.
[24] Y. Rubin, Stochastic modeling of macrodispersion in heterogeneous media, Water Resour. Res. 26 (1990) 133.
[25] P. Spanos, R. Ghanem, Stochastic finite element expansion for random media, J. Eng. Mech., ASCE 115 (1989) 1035.
[26] D.M. Tartakovsky, S.P. Neuman, Z. Lu, Conditional stochastic averaging of steady state unsaturated flow by means of Kirchhoff transformation, Water Resour. Res. 35 (1999) 731.
[27] C.L. Winter, C.M. Newman, S.P. Neuman, A perturbation expansion for diffusion in a random velocity field, SIAM J. Appl. Math. 44 (1984) 411.
[28] D. Xiu, G.E. Karniadakis, Modeling uncertainty in steady state diffusion problems via generalized polynomial chaos, Comput. Methods Appl. Mech. Eng. 191 (2002) 4927.
[29] D. Zhang, Numerical solutions to statistical moment equations of groundwater flow in nonstationary, bounded heterogeneous media, Water Resour. Res. 34 (1998) 529.
[30] D. Zhang, Stochastic Methods for Flow in Porous Media: Coping with Uncertainties, Academic Press, San Diego, CA, 2002.
[31] D. Zhang, Z. Lu, Stochastic analysis of flow in a heterogeneous unsaturated–saturated system, Water Resour. Res. 38 (2002), 10.1029/2001WR000515.
[32] D. Zhang, C.L. Winter, Moment equation approach to single phase flow in heterogeneous reservoirs, Soc. Petrol. Eng. J. 4 (1999) 118.
[33] G.A. Zyvoloski, B.A. Robinson, Z.V. Dash, L.L. Trease, Summary of the models and methods for the FEHM application – a finite-element heat- and mass-transfer code, LA-13307-MS, Los Alamos National Laboratory, 1997.